International Journal of Heat and Mass Transfer 56 (2013) 683–693

Contents lists available at SciVerse ScienceDirect

International Journal of Heat and Mass Transfer

journal homepage: www.elsevier.com/locate/ijhmt

Onset of boiling and propagating mechanisms in a highly superheated liquid - the role of evaporation waves

Benoit Stutz [a,*], José Roberto Simões-Moreira [b]

[a] LOCIE UMR 5271, Université de Savoie – CNRS, 73376 Le Bourget du Lac Cedex, France
[b] SISEA–Alternative Energy Systems Lab, Escola Politecnica da USP, Brazil

ARTICLE INFO

Article history:
Received 11 November 2011
Received in revised form 21 August 2012
Accepted 30 August 2012

Keywords:
Boiling
Superheat
Evaporation waves
Vaporization

ABSTRACT

This paper presents experimental results of the onset of boiling in highly superheated liquids on heated surfaces. The experiments have shown that at a very high degree of superheat, the phase change takes place in an unusual way as documented by high speed motion video camera. The authors have proposed a physical model to explain the observed phenomenon in the context of evaporation waves theory and its role on the phase change that occurs in a fast moving vaporization front.

© 2012 Elsevier Ltd. All rights reserved.

1. Introduction

The present study concerns transient boiling in highly superheated liquids. The study is applied to a highly wetting fluid (*n*-pentane on copper block). A mirror finished surface was used to reach a highly superheated liquid in contact with a heated surface to study the onset of boiling and its propagating mechanism. The dynamic and the shape of the bubble developed were experimentally studied using a high speed motion video camera. The images showed that the early stage of the onset of boiling, an initial vapor bubble characterized by a smooth interface was formed on the surface. As the bubble grew, a very rough vaporization front spread out on the heated surface around the bubble forming a kind of "straw hat" structure. The velocity expansion of the vapor front was measured for different liquid superheats by analyzing the front progression seen in successive video images. The "spreading" interface corresponds to that of the front mechanism in an evaporation wave in highly superheated liquids. A rule-of-thumb expression describing evaporation waves was used to estimate parameters and to shed some light on the understanding the complex phenomenon taking place on the vaporization front.

1.1. Bubble growth

Different models have been developed in order to describe bubble growth mechanisms in superheated liquids. They have been applied to describe a bubble growth submitted to a sudden pressure decrease (cavitation) or to a temperature increase (boiling) processes. Most of them consider an infinity liquid phase medium surrounding a bubble, having volume forces neglected, and the models usually take advantage of symmetrical properties of the problem. Few of them take into account the presence of a heated surface or the slip velocity between vapor and liquid phases. In these models, three main regions characterized by specific geometrical and physical properties have to be considered: surrounding liquid (infinity medium), the vapor phase inside the bubble, and the interfacial area. Simplest models used to predict bubble growth are due to Rayleigh [1] and Plesset [2], which considers the "axisymmetric" growth of a bubble in a uniformly heated infinity liquid medium. Bubble growth is supposed to be controlled by inertial forces in the liquid phase along with surface tension. The vapor density is assumed to be negligible compared to the liquid density and the vapor pressure inside the bubble keeps constant and equal to the vapor pressure at the liquid temperature. As a result, their model shows that the growth rate of the bubble increases with time.

The influence of conduction heat transfer at the interface has been taken into account in the past by several authors, such as Bosnjakovic [3]; Plesset and Zwick [4]; Forster and Zuber [5]; Scriven [6]; and Mikic and Rohsenow [7]. The heat supplied by conduction to the liquid for the vaporization process leads to a superheat depletion near the interface at the liquid side which affects the bubble growth rate. For large Jakob numbers, the bubble radius growth is proportional to the square root of the time as it is well known in the two-phase flow literature. At the early growth stage,

* Corresponding author.
E-mail address: benoit.stutz@univ-savoie.fr (B. Stutz).

0017-9310/$ - see front matter © 2012 Elsevier Ltd. All rights reserved.
http://dx.doi.org/10.1016/j.ijheatmasstransfer.2012.08.057

Nomenclature

c_p	Specific heat at constant pressure J kg^{-1}K^{-1}
h_{lv}	Latent heat of vaporisation J kg^{-1}
h	heat transfer coefficient W m^{-2}K
J	superficial mass flow kg m^{-2}s^{-1}
Ja	Jakob number
P	Pressure Pa
$\dot{q}$	Heat flux W m^{-2}
S	Area m^2
t	Time s
T	Temperature K
U	Evaporation wave front velocity m s^{-1}
v	Specific volume m^{3}kg^{-1}
V_1	Superheated liquid velocity m s^{-1}
V_2	Two-phase velocity m s^{-1}
V	Volume m^3
W_1	Relative superheated liquid velocity m s^{-1}
W_2	Relative two-phase velocity m s^{-1}

Greek symbols

Δ	jump in property

Subscripts

e	Equilibrium conditions
imp	Imposed heat flux
v	Vapor
l	Liquid
ONB	Onset of Nucleate Boiling
sat	Saturation
w	Wall
R	Relative

bubble expansion is controlled by inertial forces just as given by Rayleigh and Plesset models. The transition to a heat conduction controlled expansion stage depends on the heat flux supplied by the interface and the thickness of the thermal boundary layer around the bubble. The consideration of the presence of a heated surface makes the problem even more complex: (1) The temperature gradient inside the boundary layer have to be considered, (2) new forces acting on the bubble behavior appear, and (3) different scale orders have to be taken into account (from micro-scales at the triple line to macro-scales). Different analytical approaches have been proposed. Han and Griffith [8] proposed a spherical growth model taken into account the heat transfer conduction into the macro-layer enveloping the upper portion of the bubble. Cooper [9] considered heat transfer inside the micro-layer and applied his model to hemispherical bubbles. The model of Srinivas and Kumar [10] assumed the shape of the bubble to be spherical considering macro and micro-layers. Stephan and Hammer [11] proposed a microlayer theory. Their theory predicts that most of the heat transferred during the boiling occurs at the micro-region of the three-phase contact line by evaporation. Because of the complexity of the problem, numerical computations have to be used to solve the micro and macro layers to predict bubble growth near heated surfaces in a 3D field. Kern and Stephan [12], proposed a quasi-stationary heat transfer model applied to single vapor bubbles to compute nucleate boiling heat and mass transfer. More recently Fuchs et al. [13] proposed a fully transient heat and fluid flow model with a free surface of the rising bubble including additional microscopic effects at the bubble base. The model enables one to evaluate the influence of the transient heat conduction, heat storage, and convection in the liquid phase as well as heat transfer at the wall on the overall heat transfer process. The bubble shape depends strongly on the liquid–vapor-surface contact angle. Chen and Groll [14] have developed a method to simulate existing bubble shapes by solving the Young–Laplace equation numerically considering the dynamic effects of bubbles growing on heated surfaces. Dynamic contact angle calculations were performed using experimental correlations. The dynamic contact angle computation is still an open problem that needs additional studies. The fully understanding of the problem is still an open question, more especially when the vaporization rate becomes very high.

Experimental observations have shown that typically for a liquid superheat lower than 20 K, bubble cap shapes can take the approximated form of smooth spheroids or ellipsoids. On the other hand, at higher liquid superheat the scenario changes dramatically. Okuyama [15]; Okuyama and Iida [16], Aktershev and Ovchinnikov [17,18] have shown still pictures of the phenomenon where one can clearly see that boiling incipience proceeds by a combination of a single smooth bubble associated with a rough propagating front near the heated wall. They also noticed that the expanding front occurs at a nearly constant growth rate. In this context the classical models do not apply to this class of problems. Some attempts have been made in literature in order to model this new physical configuration such as the ones proposed by Okuyama et al. [19], Avksentyuk and Ovchinnikov [20], [21]. An appropriate discussion of that subject is addressed in Section 4.

2. Experimental setup and test procedure

The experimental setup consists of a pool boiling cylinder vessel having 160 mm internal diameter and 150 mm height filled with saturated *n*-pentane at an 1 bar pressure (T_{sat} = 35.7 °C). A schematic diagram of the experimental device is shown in Fig. 1. The pressure was maintained constant during the experiments using an external water condenser and an auxiliary vapor generator. The test heater is a 90 mm height cylindrical copper block, insulated on its periphery by Teflon ® (λ = 0.25 W m^{-1} K^{-1}). The copper surface and *n*-pentane make a high wetting pair from the boiling point of view. Two cartridge heaters were imbedded in the copper block. The 30 mm diameter bare top surface of the copper block makes up the boiling test surface under investigation. The test surface is mirror finished (measured roughness obtained with an UBM technique indicated a *Ra* less than 0.06 μm) and mounted flush with the vessel bottom as seem in Fig. 1. The contact line between the copper block and the vessel bottom is filled with a special adhesive to avoid parasite nucleation sites. Two chromel–alumel (type K) thermocouples located at 12.2 and 47.6 mm underneath the surface are used to determine the heat flux and the wall temperature by means of an inverse heat conduction method (Raynaud [22]). Considering the installed heat insulator, heat losses at the bottom or through lateral surfaces were quite negligible. Wall temperature uncertainties are estimated to be ±0.2 K which are due to thermocouple positioning and calibration precision as well as copper thermal properties uncertainties. The heat flux accuracy in within ±0.2 W cm^{-2} for heat fluxes smaller than 5 W cm^{-2} and within ±0.5 W cm^{-2} for higher heat fluxes. The data acquisition rate is 1 Hz. The free *n*-pentane liquid level is held at approximately 90 mm above the test heater surface.

The growth of the initial bubble and its progression into the superheated liquid along the heated surface was observed using a high speed video camera. The camera was either set up laterally to the glass vessel in order to capture the side view of the phenom-

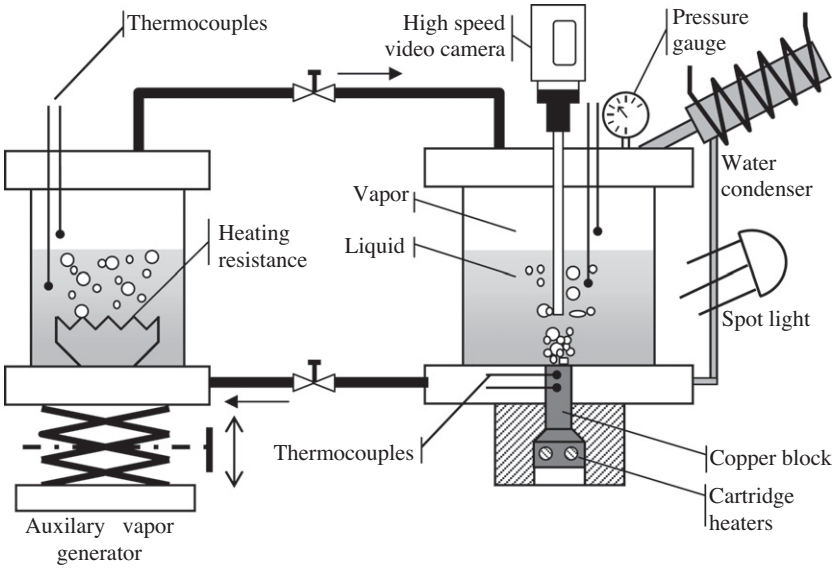

Fig. 1. Experimental setup.

enon or connected to an endoscope in order to capture the top view. Considering the geometrical shape of the vessel, the refractive indexes of the different materials located between the camera and the copper block (air, glass, *n*-pentane) and the camera inclination, the side view are only used for qualitative analysis. The endoscope could traverse vertically the top of the vessel in order to obtain a maximum camera focusing of the heated surface. Image calibration was carried out using the known dimensions of the heated surface, which enabled to compute the position of the triple line on the heated surface and thus the velocity of the vaporization front between successive images.

Two 500 W spotlights with low infrared emission were used to illuminate the surface so the high speed images could be taken. The light was switched on when the surface temperature reached 45 °C. The spotlights were directed towards the center of the heated surface and were also oriented at a 30° angle to the horizontal as depicted in Fig. 1. Considering the high infrared glass absorption and the mirror finishing heated surface, the thermal impact of the lighting on the heated surface was negligible. This assumption was verified by thermal measurements because no thermal perturbation was observed when the spotlights were switched on.

The vessel bottom was mounted on the pool boiling vessel which was connected to a vacuum pump. A pressure level approximately equal to 0.17 mbar was maintained during 12 h to ensure an accurate desorption of the system. The valves that connect the boiling vessel to the auxiliary vapor generator (Fig. 1) were kept closed. Next, *n*-pentane was allowed to flow into the boiling vessel. Vigorous boiling was imposed to the fluid during nearly 2 h. During that period, the vapor was condensed in order to maintain the pressure level above 1.2 bar and any non-condensable gas was eliminated by regular draining of the condenser. After that preliminary procedure, the *n*-pentane was maintained at a temperature of 36.5 °C (P_{sat} = 1 bar) to prevent any non-condensable gas entry. Now, the boiling experiments could start off.

Once the system temperature has been set up, the copper block was cooled by a water heat exchanger put in contact with the copper block bottom until the liquid next to the test surface was 10 K subcooled. Next, the water heat exchanger was removed immediately before a test starts. Then, a stepwise heat flux was imposed as indicated by the dashed line in Fig. 2 at the time t = 100 s. The heat flux imposed at the base of the copper block $\dot{q}_{imp}$was kept

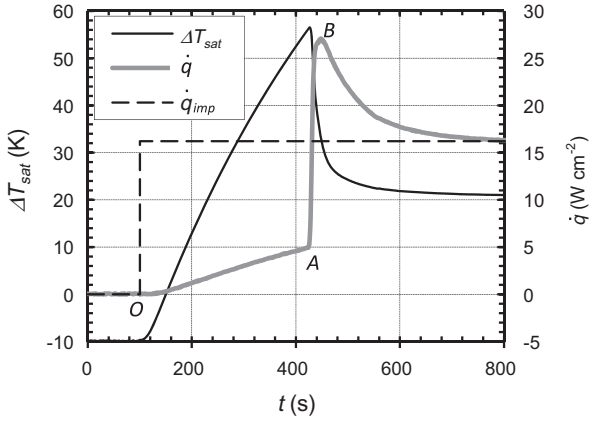

Fig. 2. Transient superheat and heat flux versus time for stepwise heat generation of 50% CHF supplied to the cartridge heaters.

constant throughout an experiment run at 16 W cm^{-2}, which was nearly 50% of the critical heat flux (32 W cm^{-2}). The thicker line in Fig. 2 indicates the heat flux transferred from the heated surface to the liquid. At early stages (O–A), heat was transferred by free convection and a cell type liquid motion was observed by naked eyes upon the heated surface. The wall superheat and the heat flux transferred to the liquid increased in an almost linear fashion and, consequently, the heat transfer coefficient was nearly a constant, whose value corresponded to the one measured at steady-state conditions ($h \approx 890$ W m^{-2}K^{-1}). At this initial free convective regime, the transient temperature increased at a rate around 0.25 Ks^{-1}, as indicated by the thin line in Fig. 2. Boiling started in an almost explosive manner around 320 s after the beginning of the heating step. The superheat at the wall was about 56 K and the surface heat flux was about 5 W cm^{-2} just before triggering the phenomenon. Then, suddenly the whole phenomenon started off, and it was noticed a jump in heat flux transferred to the fluid, which corresponds to the almost vertical line (A-B) in Fig. 2. At the same time there was a steep superheat drop (thin line in Fig. 2). Further analyses of the high speed motion pictures indicate the formation of a single large bubble. Next the bubble grew very rapidly covering over the entire heated surface. Depending on the superheat degree and the Leidenfrost temperature, the phenomena can

evolve to either to pool boiling regime or film boiling regime. Transition to film boiling could occur if the surface superheat was above the Leindenfrost temperature (the superheating of the Leidenfrost point $\Delta T_{\text{Leidenfrost}}$ has been determined experimentally by Stutz et al. [23] and it was about 60 K). It has been observed in a few experiments the direct transition to film boiling but that is not the case observed in this work. Experimental conditions presented in this study led systematically to nucleate boiling regime transition after boiling incipience.

After boiling incipience, vigorous boiling was maintained during 5 min before switching off the power supply. The water heat exchanger was then attached again to the bottom of the copper block in order to impose a 10 K subcolling to the liquid at the heated surface and to flood all the nucleation sites that contains pure vapor. Heated surface subcooling was imposed during nearly 10 min before a new experiment starts.

3. Experimental results

The superheat ΔT_{ONB} at onset of boiling increases with cycling number (Fig. 3). It starts at around 40 K and then increases regularly up to reach about 55 K after about 15 cycles. The onset of boiling temperature then randomly clustered around 55 K. Besides the cycling test, it was also investigated the influence of the heat flux imposed to the copper base $\dot{q}_{imp}$ from 20 to 80% of the critical heat flux $\dot{q}_{crit}$. As seen in the graphics in Fig. 3, the imposed heat flux did not have any noticeable influence. Finally, the boiling period, the subcooling period between two experiments, and the subcooling temperature itself varied from 5 to 12 K and they altogether did not show any noticeable influence over the results. Therefore, the spreading of the onset of boiling temperature seen in Fig. 3 is to be found yet, and the spreading cannot be associated with those mentioned parameters.

The homogeneous nucleation superheat can be estimated using the rate of formation of vapor nuclei critical size per volume unit within the bulk of a pure liquid. The homogeneous nucleation superheat for *n*-pentane at atmospheric pressure leads to a temperature about 153 °C as given by the standard theory ($J = 10^{12}$ m^{-3} s^{-1}) which is much higher than the T_{ONB} = 91 °C obtained in the present experiments. Because *n*-pentane is a highly wettable fluid in copper surfaces, the homogeneous nucleation value can be used as a reference value for evaluating the temperature on a perfectly smooth surface (Duluc et al. [24]). On the other hand, heterogeneous nucleation can be initiated from cavities, scratches or impurities embedded on the surface. As a conclusion, for liquid *n*-pentane, an incipient superheat as low as 50 to 60 K may result from the activation of pre-existing vapor embryos entrapped in the cavities.

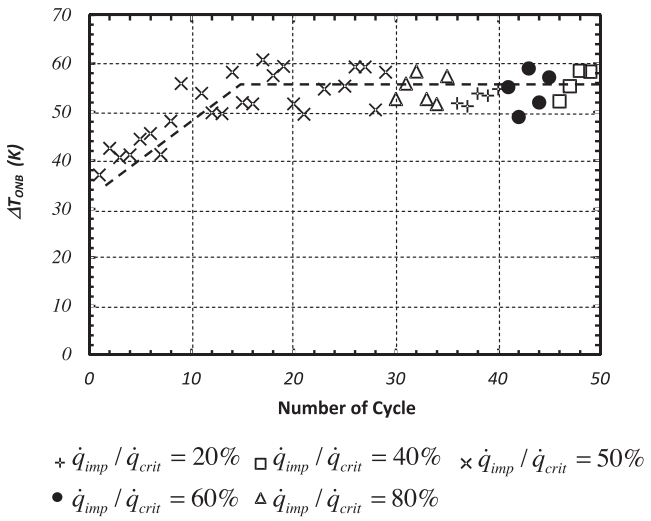

Fig. 3. Evolution of the superheat at onset of boiling with the number of cycle.

As mentioned in Section 2, the temperature of the heated surface increased slowly during the free convection regime. The heat transfer coefficient is similar to the one measured at steady-state conditions as shown by Cances [25]. Steady-state simulations show the presence of a toroid vortex cell in the liquid and a boundary layer with a thickness increasing from 0 at the periphery of the heated surface to the liquid layer thickness in the center of the heater corresponding to the symmetry axis of the vortex. Considering that the equilibrium bubble radius is of the order of tenths of micrometer, thus the thermal boundary layer thickness is order of magnitudes greater. Therefore the thermal boundary layer can reasonably be considered to have no influence on boiling incipience. This can explain why the temperature of onset of boiling is not a function of the heat flux imposed to the copper block as indicated in Fig. 3.The boiling incipience site usually changes from one cycle to the other which may explain the spreading of the onset of boiling temperature seen in Fig. 3.

Image sequences in Figs. 4 and 5 are respectively top and side views of the boiling incipience, the growth of the initial bubble and the spreading of the vaporization front on the superheated surface. These images were taken with the high speed motion camera and the proper time sequence is shown underneath each picture and they do not correspond to the same boiling incipience cycle because the camera had to be setup for each view. One can see that the boiling incipience sites are different. In Fig. 4 (top view) boiling started near the heated surface center whereas in Fig. 5 (side view), boiling started off center. There is no special reason for that, since boiling incipience occurred randomly in other tests. Whatever the boiling incipience location was, it was seen a formation of an initial vapor bubble characterized by a smooth interface at the early stages ($t \leqslant 16$ ms). At this stage the rising velocity due to buoyancy forces is low compared to its growth rate (dr/dt), which leads to a hemispheric expansion of the bubble. One can also observe at the same time the formation of a very rough vaporization front spreading out on the heated surface around the bubble. As time increases, the bubble growth rate decreases and as a consequence the rising velocity becomes more significant compared to its growth rate. The bubble shape becomes spherical and the main central bubble detached from the surface about 56 ms after the boiling incipience. The growth rate of the bubble cannot be determined using the top view images because of image distortion. The vaporization front that spreads out on the heated surface seems to be made of a many coalesced bubble of milimetric size. The propagating front envelopes the main vapor bubble whatever the position of the boiling incipience location was. It was also observed that the propagating front velocity was approximately uniform. The vaporization front stops when it reaches the border of the heated surface.

The contour of the vaporization front as it progresses is depicted in Fig. 6. The contour lines seen in that figure where obtained from a 2 ms time step successive top view images. As one can see, there is a very irregular spreading front enveloping the initial central nucleation site but it is also possible to identify an approximately circular concentric spreading front. For each contour line one can associate a periodic 3.5 mm wave length on the contour itself for this experiment. The question of the mechanism governing the expansion of the vaporization front is still open and will be discussed in Section 4.

From the analysis of Fig. 6, it is possible to compute the time rate evolution of the expansion of the vaporization front from the initial central nucleation site in different directions. In Fig. 7 it is shown the expansion radius taken at three different directions: 0, 90, and 180° from an imaginary horizontal reference line seg-

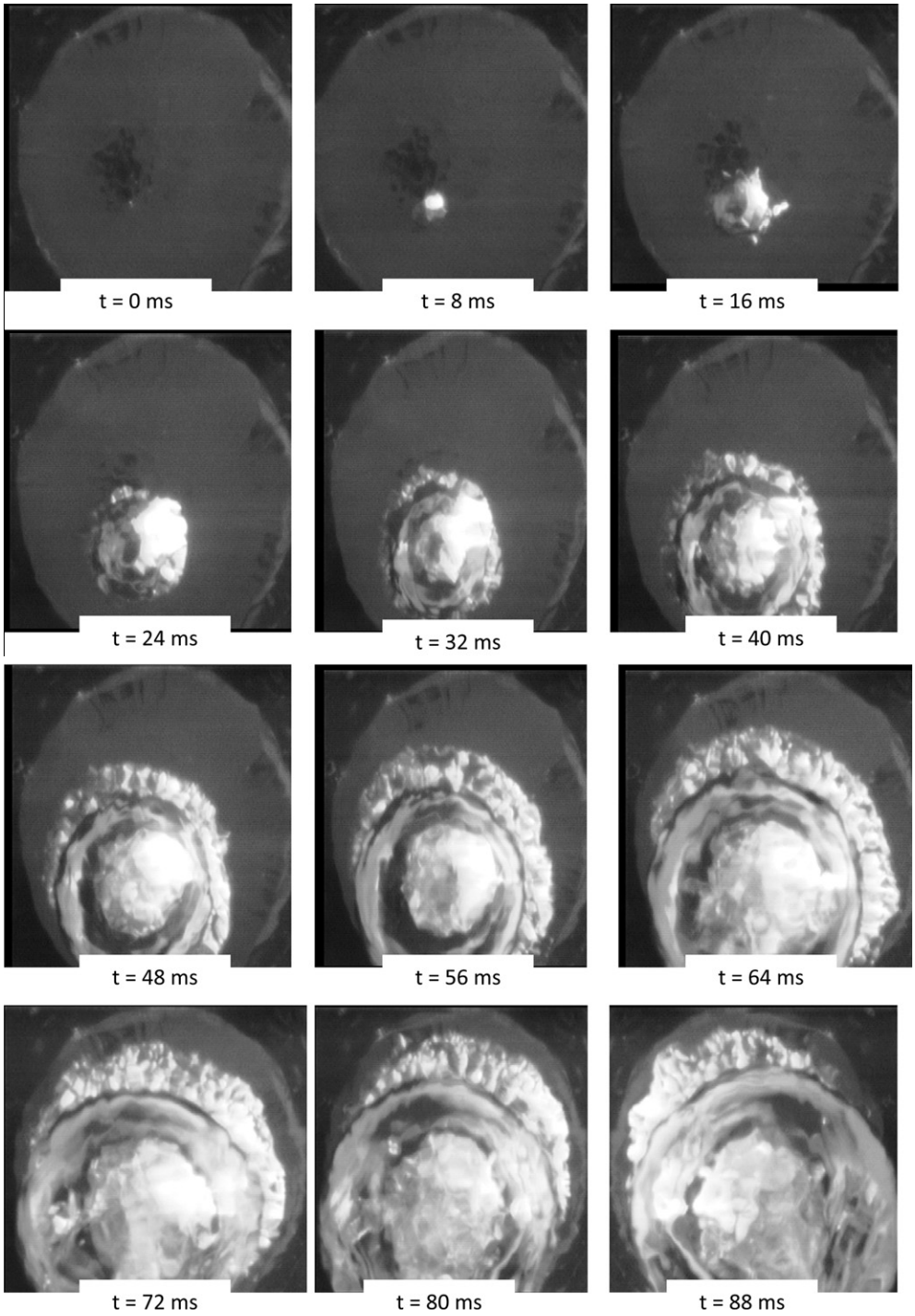

Fig. 4. Sequence of images describing the onset of boiling - top view.

ment in that figure centered at the initial nucleation site. As we can see, there is an average linear expansion in those three directions, which also represents the radial expansion in all directions. The slope of that line is the time average velocity of the vaporization front. However, the instantaneous velocity fluctuates around that average value around a mean value equals to 0.1 m/s for the case displayed in Fig. 7. The period of the instantaneous velocity oscillation is about 40 ms. The wave length computed using the average velocity of the vaporization front and this velocity oscillation period is about 4 mm, which is surprisingly similar to the wave length of the contour itself as mentioned previously. No conclusion could be found to explain that behavior.

In Fig. 8 it is shown the average velocity obtained using the procedure just described in the previous paragraph as a function of the onset of boiling superheat. The standard deviation of the velocity is also reported in the same figure as vertical deviation bars. The standard deviation indicates the instantaneous velocity fluctuation around the average velocity for each experiment.

As a general rule, the mean velocity of the vaporization front increases with the increase of the onset of boiling superheat. However for the same onset of boiling superheat, different average velocities could be observed, which means that other factors may also affect the phenomenon. For instance, the location of the initial nucleation does not have any influence at all over the velocity.

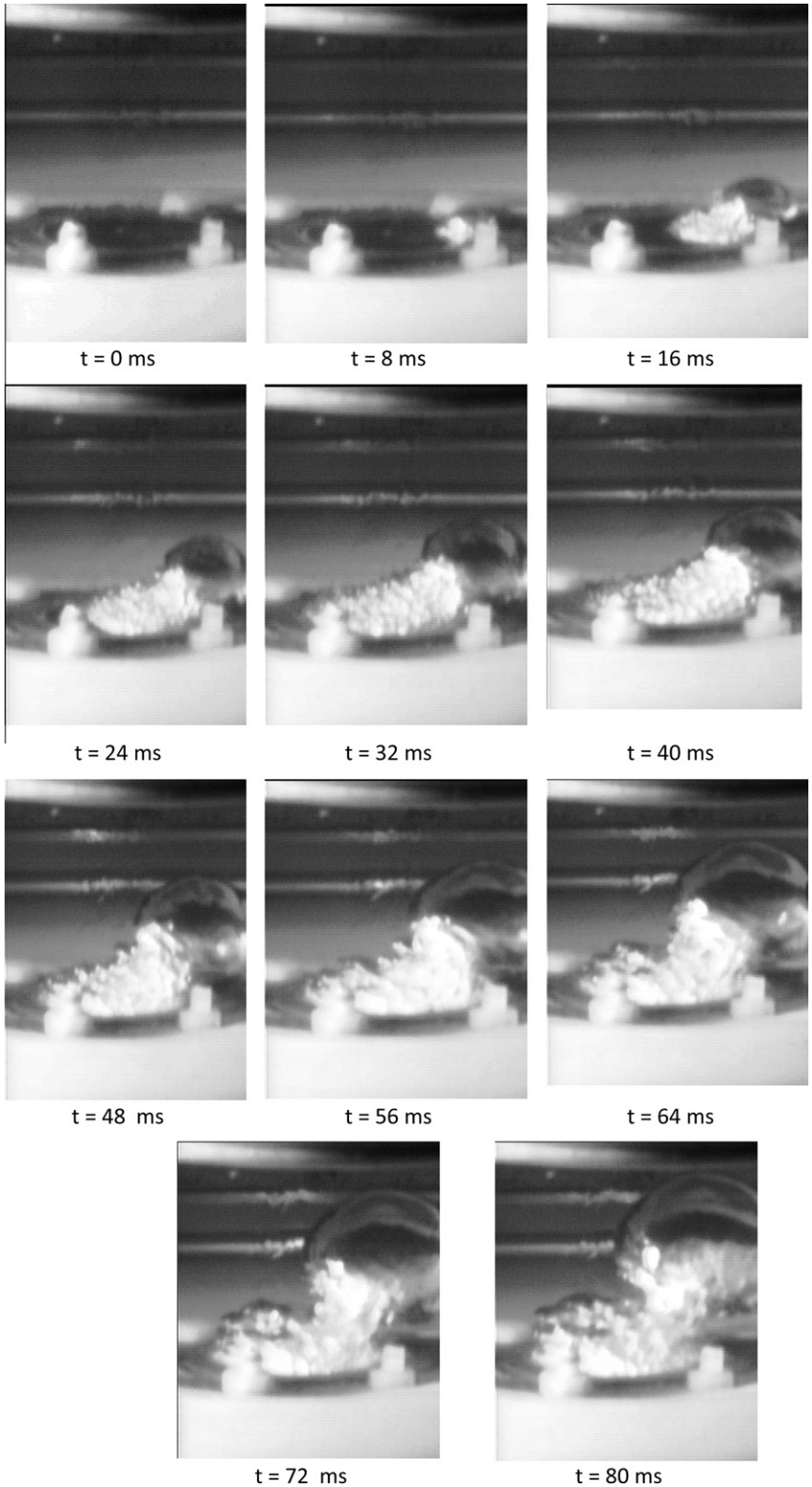

Fig. 5. Sequence of images describing the onset of boiling - side view.

4. A novel contribution to elucidate the phenomena

In this section it is presented a novel contribution to elucidate the phenomena that occur on the phase transition following the onset of boiling for highly superheated liquids. As discussed in the introductory section, the classical bubble growth model does not capture the phase change features observed in laboratory as describe in Section 3 as well as in other experiments in similar configuration available in the literature [15,18].

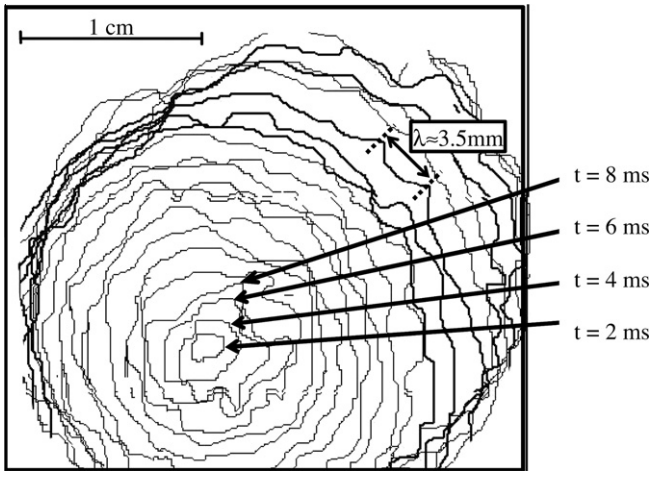

Fig. 6. Evolution of the vaporization front during a boiling incipience cycle.

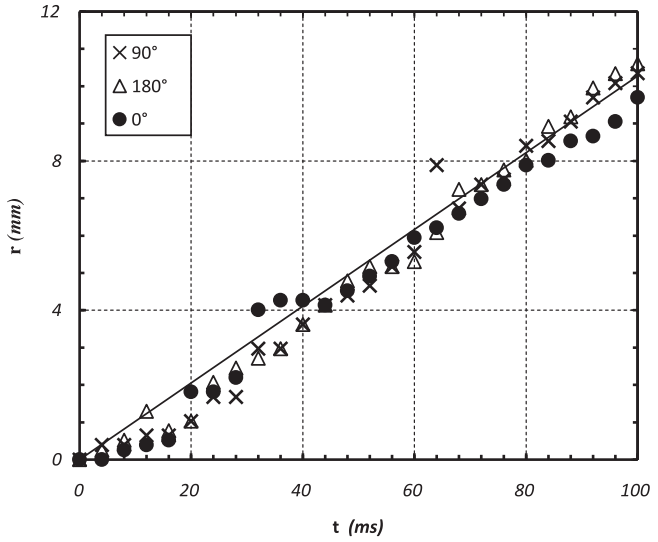

Fig. 7. Time evolution of the distance of the vaporization front from the point of boiling incipience on a given radius.

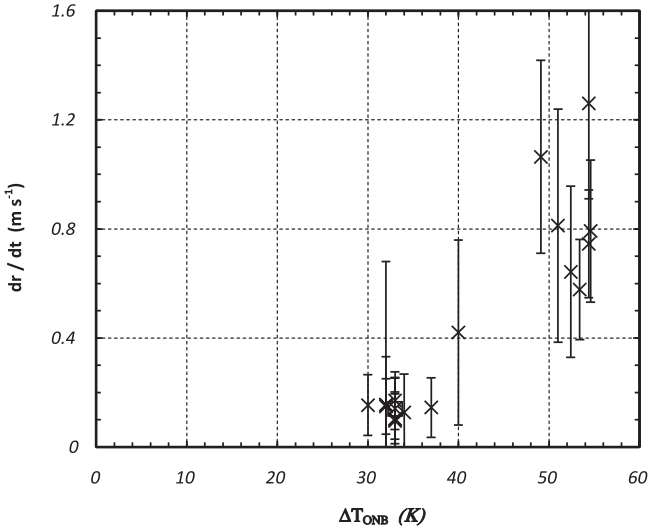

Fig. 8. Impact of the superheat at onset of boiling on the time average velocity of the vaporization front.

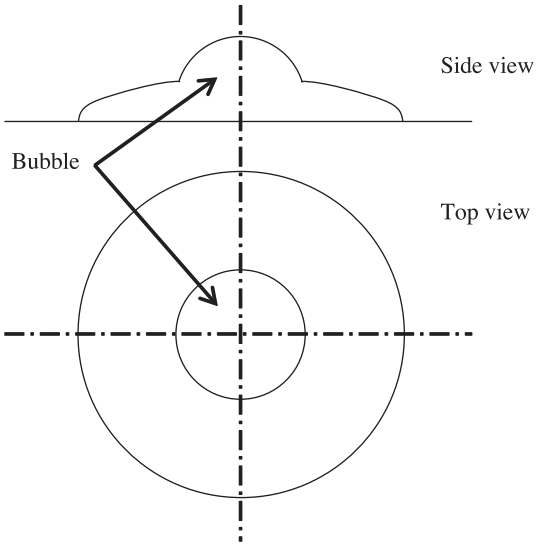

Fig. 9. Physical description according to Okuyama and Iida [16].

4.1. Previous contributions and models

Okuyama and Iida [16] proposed a fancy description of the phase change process suggesting the term "straw hat" structure due to its resembling similarity as pictorially illustrated in Fig. 9. Their first assumption is to divide the observed phase change process in two parts according to the experimental observations: (a) The "hat crown" is formed by a smooth sector spheroid bubble that initially grows on the surface up to a certain stage and then the nucleation is triggered surrounding the initial bubble to give rise to the "hat brim" structure; (b) The "hat brim" is a phase change process that propagates in all radial directions into the superheated liquid.

Avksentyuk and Ovchinnikov [21,26,27] have proposed a physical model which is reproduced in Fig. 10. According to their model, there is a smooth propagating front running next to the solid surface as illustrated in that figure. Superheated liquid (label "0") undergoes a complete phase change through an evaporation front resulting in a pure downstream vapor (label "1"), i.e., a complete phase change process. As usual in analyses of discrete evaporation fronts (Labuntsov and Avdeev [28,29]; Simões-Moreira [30,31]; Simões-Moreira and Shepherd [32]), those authors [26,27,21] write down the 1-D version of the three conservation equations (mass, momentum and energy) in a moving reference frame attached to the evaporation wave. However, they introduced capillarity effects by including the surface tension in the momentum balance equation. Also, they assumed that the liquid motion around the smooth tip (stream lines in Fig. 10) supplies convective heat to the evaporating front.

Later Okuyama et al. [33] drew attention to the fact that there are two possible mechanisms to explain the "hat brim" propagation. The first one considers that bubbles are activated in the region adjacent to the moving front and there occurs coalescent growth of nucleated bubbles. The second one considers a smooth propagating front next to the wall as proposed by Avksentyuk and Ovchinnikov [27] and described above.

4.2. Proposed model

The physical model proposed in this paper is somewhat different from Avksentyuk and Ovchinnikov's [26,27] smooth propagating front near the wall, but it can be considered as an improvement

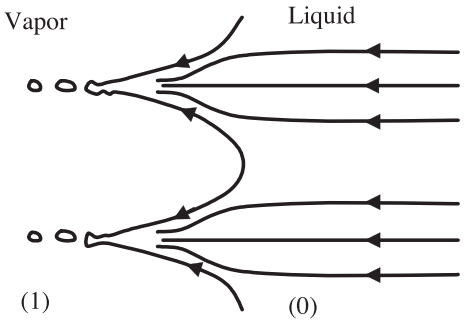

Fig. 10. Physical description according Avksentyuk and Ovchinnikov [27].

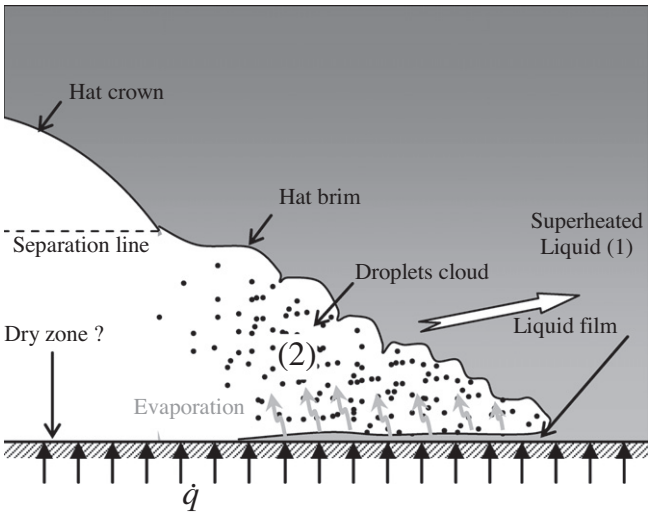

Fig. 11. Physical modeling of the phenomenon.

of the Okuyama's phenomenological description. The former authors' model fails to explain what the pictures obtained experimentally have shown, i.e., that there exists a very "rough" peripherical phase change interface spreading out into the superheated liquid from a central smooth spheroidal cap as seen in Figs. 3 and 4 as well as the schematics contours in Fig. 6. The present model is a combination of the classical bubble growth theory along with evaporation waves. A pictorial view of the physical model is presented in Fig. 11. According to the authors' observations (Figs. 3 and 4), a smooth spheroidal sector ("hat crown") is surrounded by a layer of small spheroidal bubbles propagating into the superheated liquid in all directions dominated by a parallel motion near the heated copper block surface at an average radial velocity as shown in Fig. 7 and discussed in Section 3. Bubbles have a life time formed by small vapor embryo trapped into the superheated liquid, growth, and burst process in such a way that open and semi-open spheroidal shapes are also present in the vaporization front as depicted in Fig. 11.

The description of the "spreading" interface corresponds exactly with that of the front mechanism in an evaporation wave in highly superheated liquids as, for instance, documented and described in Ref. [30,32]. Evaporation waves are adiabatic phase change processes in which a superheated or metastable liquid undergoes a sudden evaporation in a shock-like process, that is, the phase change is confined to a discrete and observable zone, which moves into the undisturbed superheated liquid and a two-phase mixture is observed downstream of the wave front. A still picture of an evaporation progress is shown in Fig. 12.

An important feature of evaporation waves is that such adiabatic phase change process cannot result in a complete phase

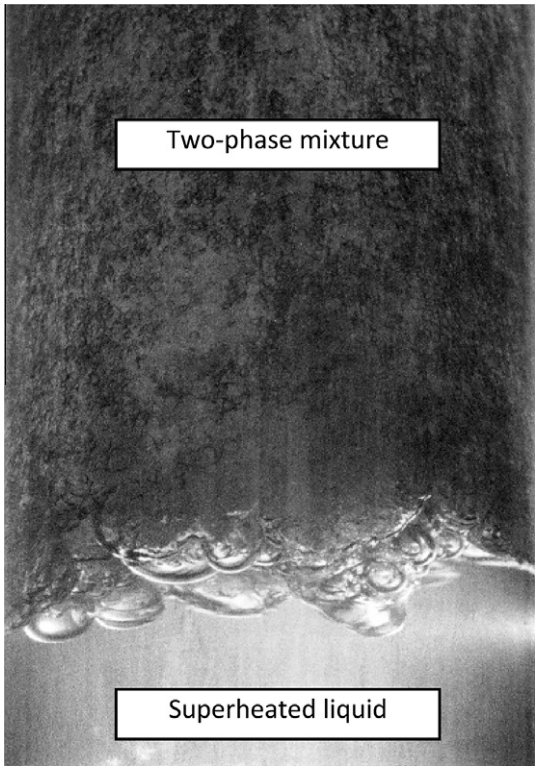

Fig. 12. Image of an evaporation wave in progress [29].

change, i.e., a process that would result in only pure vapor downstream of the evaporating wave front. For the hydrocarbon series, it has been estimated (Shepherd et al. [34]) that a complete evaporation wave, i.e., an adiabatic evaporation from superheated liquid to a pure downstream vapor would take place for hydrocarbon molecules that are formed by 8 or more carbon atoms per molecule. Therefore, octane (C_8H_{18}) is the hydrocarbon molecule that fulfills the minimum necessary requirement. In fact, Simões-Moreira et al. [35] carried out a theoretical analysis in order to establish the thermodynamic requisites for obtaining a complete evaporation and they used dodecane ($C_{12}H_{26}$) as a study case example. Later, laboratory experiments showed that an estimated vapor quality above 90% was obtained in tests with superheated dodecane in 1-D experiments [30,32]. Therefore complete evaporation of regular testing substances such as *n*-pentane, water, toluene and R-113 cannot be obtained without heat being supplied to the vaporization front. Substances that can achieve a complete phase change through evaporation waves have been known as "retrograde" [36]. If heat is supplied to the vaporization front as proposed by other authors, the process cannot proceed in a constant velocity as observed in the present experiment (Fig. 7) as well as in the works of Avksentyuk and Ovchinnikov [26,27] and Okuyama and Iida [16].

The whole description of the phenomenon is as follows: Following the inception and growth of a single smooth bubble according to the classical model, the initial smooth bubble will grow up to a certain stage and then a combination of some surface finishing and liquid superheat will trigger a front of evaporation characterized layers of small bubbles at a rapid growth rate, coalescence, and burst which forms the evaporation wave front as illustrated in Fig. 11. Pictures from the high speed motion camera (Figs. 4 and 5) also show open and semi-open spheroid structures in that evaporating front which can be an indication of bubbles life time. The evaporation wave front will propagate in all directions as illustrated in Fig. 6 from the original bubble. Due to the thermal boundary layer

next to the wall, an evaporation wave front will proceed into the superheated liquid at different degrees of superheat, being the superheated liquid at the highest degree next to the wall and the lowest degree, or none, at the thermal boundary layer thickness (Fig. 11). Therefore, once the evaporation wave front has being triggered and started off it will run into the superheated liquid to form the downward curved "hat brim" as described by Okuyama and Iida [16], also illustrated in Fig. 9, and documented in Fig. 5. At the same time, the original smooth bubble has grown to form the "hat crown" at a distance from the wall of the same order as the thermal boundary layer thickness and then it will undergo a side growth or "stretching" due to the mass inflow from the evaporation wave front. The cap of this smooth spheroidal structure is dominated by capillary forces and mechanical equilibrium dictates the inside pressure near the "hat crown" cap must be the same as the liquid pressure plus the pressure corresponding to the surface tension as given by the Laplace equation.

Keeping Fig. 11 in mind, one can see that a smooth spheroidal sector is connected to the evaporation wave front by a "separation line", whose height from the surface is of the same order as the original thermal boundary layer thickness as a first approach. The evaporation wave front into the liquid ("hat brim") is moving into the superheated liquid. As a consequence, the upstream superheated liquid (label "1") undergoes an adiabatic phase change process via an evaporation wave originating the downstream two-phase flow (label "2"). The figure also illustrates that not all the superheated liquid will evaporate and some small droplets will also be formed that may fall on the hot surface in accordance with the above non-retrograde character of the tested substances. In order to investigate in more details the evaporation wave front, a control volume (CV) approach enveloping the wave can be used as illustrated in Fig. 13.

Fig. 13 shows two control surfaces (CS) limiting the evaporating wave front at both sides and the thickness between them is such that uniform properties are assumed in either side. On solving this sort of problems it is also a convention to work on a moving reference frame in which the evaporation wave front is stationary in relationship to the laboratory frame. Actually, the evaporation wave front is moving at an instantaneous and local velocity, $\vec{U}$. The upstream and downstream relative velocities are also shown in figure. On this moving reference frame, one can picture that a superheated liquid flows into the CV at a relative velocity, $\vec{V}_{R1}$, and a two-phase mixture leaves the CV at a relative velocity, $\vec{V}_{R2}$. The figure also shows the normal components $\vec{W}_1$ and $\vec{W}_2$ respectively for the superheated liquid and the two-phase mixture and the tangential velocity component $\vec{t}$, which is invariant across the discontinuity. The downstream mathematical solution for a given upstream condition can be achieved by solving the adiabatic jump equations with appropriate downstream boundary conditions for an oblique evaporation wave [31]. It is noteworthy to mention that a local and instantaneous solution must be obtained, since the upstream superheated liquid temperature varies according to the degree of superheat caused the thermal boundary layer in a perpendicular to wall position. Local solution means that the degree of liquid superheat is a function of the y distance from the wall and it will lead to different evaporation wave downstream solutions accordingly.

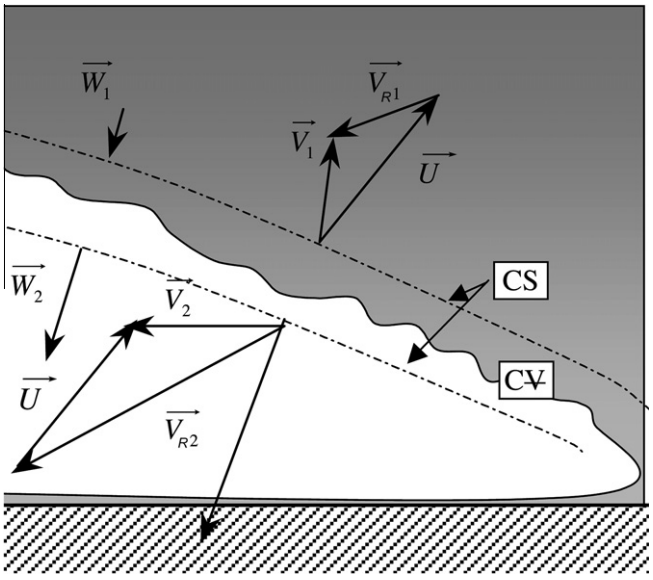

Fig. 13. Control volume around the evaporation wave front.

Experimental observations on evaporation waves [30,32,37] show that there is a cloud of droplets leaving the evaporation wave front. In the present model the droplets leaving the evaporation wave front will impinge on the hot surface to form a liquid film, as depicted in the pictorial illustration in Fig. 11, if the test surface temperature is lower than the Leidenfrost temperature. Of course, the liquid film thickness will depend on the vapor quality of the downstream flow and the impinging liquid vaporization at the wall. On impinging on the surface, a simultaneous heat and mass transfer will take place and part of the liquid film will vaporize, as illustrated. If enough conductive heat flux is provided from the wall and the amount of liquid is not too high, a dry zone will be formed around the wall center line.

Because of the thermal boundary layer, the evaporation wave front penetration into the superheated liquid will cease at and beyond the thermal boundary layer thickness δ_{TH}. Actually, for low degree of superheat, an evaporation wave phenomenon is quite unstable [30,32]. There is a threshold or minimum amount of liquid superheat for the evaporation wave to be a stable and self-sustainable phenomenon. So, there is a distance from the wall, δ_C, which one can assume to be approximately of the same order of δ_{TH} or less, for which the evaporation wave ceases and it starts the smooth sector spheroid bubble. The joining line between the two formations is indicated in Fig. 11 and it has been named as the "separation line".

Boundary conditions play an important role on the problem. The superheated liquid is set into motion because as the "straw hat" structure grows in volume it also displaces the surrounding liquid accelerating it to a local velocity, $\vec{V}_1$, ahead of the evaporation wave front. The displaced liquid velocity is both time-dependent, as it depends on the structure growth rate, and it is also space-dependent, as it depends on the "straw hat" shape. So, the actual measured velocity in laboratory experiments is the sum of the displaced liquid velocity, $\vec{V}_1$, and the evaporation wave front, $\vec{U}$, being the difference between those two magnitudes the relative velocity, $\vec{V}_{R1}$. The normal component of the relative velocity, W_1, is used to solve the conservation jump equations.

The phenomenon is somewhat complex because it couples the heat and mass transfer problem on the heated surface, the displaced superheated liquid motion just mentioned and the evaporation wave. In order to have some orders of magnitude, a rule-of-thumb expression can be used to predict the evaporation wave velocity U and the pressure jump ΔP across the vaporization front (Simões-Moreira [30,38]). For using that expression, some assumptions must be taken into account, which are only roughly valid for the problem in study. Firstly, one must assume that the tangential velocity components are negligible. Secondly, the displaced liquid velocity is negligible. Finally, the liquid–vapor mixture downstream the vaporization front is saturated at the surrounded liquid pressure and the vapor phase is an ideal gas. The relationship between the pressure jump and the velocity is given by Eq. (1):

Table 1
Estimations of the pressure jump for three onset of boiling superheat.

ΔT (K)	U (m s^{-1})	x	V_2 (m s^{-1})	ΔP (bar)
30	0.15	0.193	6.0	0.006
40	0.3	0.257	16.1	0.030
50	0.8	0.321	53.7	0.262

$$\frac{\Delta P}{U^2} = \frac{v_v Ja}{v_l^2} \tag{1}$$

where v_v, h_{lv} are taken at saturation temperature, while v_l,c_{pl} are taken at the liquid temperature. and Ja is the Jakob number defined by eq. (2):

$$Ja = \frac{c_{pl}\Delta T}{h_{lv}} \tag{2}$$

It is noteworthy to say that Jakob number is about the same as the mass vapor quality x [30,38].

Table 1 shows some rough estimations based on Eqs (1), (2) of vapor quality, two-phase flow velocity and the pressure jump for three onset of boiling superheat tested taken from the graphic in Fig. 8 along with the corresponding measured propagation front velocity U.

As seen in Table 1, it is expected to have a non-negligible amount of liquid phase downstream of the vaporization front as given by the low mass vapor quality x that will fall on the heated surface inside the bubble. At a low superheat, the pressure jump is almost negligible, but at highest tested superheat (50 K) the pressure jump is quite significant. Two-phase velocity is also high downstream the vaporization front compared to the moving front velocity. Considering the presence of small droplets leaving the front and the reduction of the sound velocity in two-phase flow compared to one in single phase flow, the downstream two-phase flow velocity could reach the sonic velocity at extreme conditions as it appears to be the case for the highest tested superheat. Such phenomena were observed in an evaporation wave in highly superheated liquids as described by Simões-Moreira and Shepherd [32].

5. Conclusions

At a high degree of liquid superheat a phase change process can occur on mirror polished heated surfaces that it is quite complex and not fully understand yet. Experiments have shown that the classical bubble growth geometry does not occur in such situations. Instead, following an initial nucleation site a single bubble is seen at the very early stage, then it is followed by a phase change process that spreads around that initial bubble into all directions on the heated surface. Okuyama [16] has named this structure as a "straw hat structure" because of the resemblance. In this paper it is proposed a physical model to explain the whole phase change problem based on the theory of evaporation waves. The evaporation wave theory in its very simplified version can give a simple relationship expression connecting the front velocity and the pressure jump (Eq. (1)). The whole problem is coupled with, at least, three physical phenomena: (1) the vaporization front can be seen as an evaporation wave as studied by Simões-Moreira and Shepherd [32]; (2) in the vaporization front the superheated liquid is partially vaporized and the remaining liquid form droplets that impinge on the hot surface that can undergo partial phase change also depending on the heat flux; (3) the "straw hat" structure growth pushes the superheated liquid and sets it into motion modifying the flow field around it. Therefore, steady state Bernoulli equation should not be applicable in the vicinity of the vaporization front. The solution of the coupled problem needs to set all equations and solve them numerically.

References

[1] Lord Rayleigh, On the pressure developed in a liquid during the collapse of a spherical cavity, Philos. Mag. 34 (1917) 94–98.
[2] M.S. Plesset, The dynamics of cavitation bubbles, ASME-J. Appl. Mech. 16 (1949) 228–231.
[3] F. Bosnjakovic, Verdamfung Flussigheitsuberhitzung, Tech. Mech. Thermodynam. (1) (1930) 358.
[4] M.S. Plesset, S.A. Zwick, The growth of vapor bubbles in superheated liquids, J. Appl. Phys. 25 (4) (1954) 493–500.
[5] H.K. Forster, N. Zuber, Growth of a vapor bubble in a superheated liquid, J. Appl. Phys. 25 (4) (1954) 474–478.
[6] L.E. Scriven, On the dynamics of phase growth, Chem. Eng. Sci. 10 (1–2) (1959) 1–13.
[7] B.B. Mikic, W.M. Rohsenow, A new correlation of pool boiling data including the effect of heating surface characteristics, J. Heat Transfer (91) (1969) 245–260.
[8] C.Y. Han, P. Griffith, The mechanism of heat transfer in nucleate pool boiling-Part 1: Bubble initiation, growth and departure, Int. J. Heat Mass Transf. 8 (6) (1965) 887–904.
[9] M.G. Cooper, The microlayer and bubble growth in nucleate pool boiling, Int. J. Heat Mass Transf. 12 (8) (1969) 895–913.
[10] N.S. Srinivas, R. Kumar, Prediction of bubble growth rates and departure volumes in nucleate boiling at isolated sites, Int. J. Heat Mass Transf. 27 (8) (1984) 1403–1409.
[11] P. Stephan, J. Hammer, A new model for nucleate boiling heat transfer, Wärme- und Stoffübertragung 30 (1994) 119–125.
[12] J. Kern, P. Stephan, Theoretical model for nucleate boiling heat and mass transfer of binary mixtures, ASME-J. Appl. Mech. 125 (2003) 1106–1115.
[13] T. Fuchs, J. Kern, P. Stephan, A transient nucleate boiling model including microscale effects and wall heat transfer, J. Heat Transfer 128 (12) (2006) 1257–1266.
[14] Y. Chen, M. Groll, Dynamics and shape of bubbles on heating surfaces: A simulation study, Int. J. Heat Mass Transf. 49 (2006) 1115–1128.
[15] K. Okuyama, Transient boiling heat transfer characteristics, R 113 at large stepwise power generation, Int. J. Heat Mass Transf. 31 (1988) 2161–2174.
[16] K. Okuyama, Y. Iida, Premature transition to film boiling at stepwise heat generation, Heat Transf. Jpn. Res. 21 (3) (1992) 317–329.
[17] S.P. Aktershev, V.V. Ovchinnikov, Dynamics of a vapor bubble in a nonuniformly superheated fluid at high superheat values, J. Eng. Thermophys. 16 (4) (2007) 236–243.
[18] S.P. Aktershev, V.V. Ovchinnikov, Vapor bubble growth at the surface of flat and cylindrical heaters, J. Eng. Thermophys. 17 (3) (2008) 227–234.
[19] K. Okuyama, Y. Iida, T. Kato, Premature transition to film boiling at stepwise heatgeneration 2nd Report: Effect of wall material and surface condition, Heat Transf. Jpn. Res. 25 (1996) 51–63.
[20] B.P. Avksentyuk, V.V. Ovchinnikov, Shape of the vapor bubble upon explosive boiling, J. Appl. Mech. Tech. Phys. 41 (2) (2000) 1070–1076.
[21] S.P. Aktershev, V.V. Ovchinnikov, Model of steady motion of the interface in a layer of a strongly superheated liquid, J. Appl. Mech. Tech. Phys. 49 (2) (2008) 194–200.
[22] M. Raynaud, Influence of convection on the boiling curves of liquid nitrogen estimated around the periphery of a rotating disk, Proceedings of the Third UK National Conference, Incorporating 1st European Conference on Thermal Sciences, ETS (1992) 147-153.
[23] B. Stutz, M. Lallemand, F. Raimbault, J.C. Passos, Nucleate and transition boiling in narrow horizontal spaces, J. Heat Mass Transfer 45 (2009) 929–935.
[24] M.C. Duluc, B. Stutz, M. Lallemand, Transient nucleate boiling under stepwise heat generation for highly wetting fluids, Int. J. Heat Mass Transfer 47 (2004) 5541–5553.
[25] J. Cances, Etude expérimentale des phénomènes de déclenchement de l'ébullition, Master Dissertation, DEA thermique, INSA Lyon, (2002) 70 p.
[26] B.P. Avksentyuk, V.V. Ovchinnikov, Dynamics effects on interphase surface during the disintegrationof superheated nearwall liquid, Proceedings of International Center of Heat and Mass Transfer, 33 (1991) 583-598.
[27] B.P. Avksentyuk, V.V. Ovchinnikov, Dynamic of explosive boiling of drops at the superheat limit, J. Appl. Mech. Tech. Phys. 40 (6) (1999).
[28] D.A. Labuntsovand, A.A. Avdeev, Theory of boiling discontinuity, Teplofiz. Vys. Temp. 19 (1981) 552–556.
[29] D.A. Labuntsov, A.A. Avdeev, Mechanism of flow blockage involving shock boiling of liquids, Teplofiz. Vys. Temp. 20 (1982) 88–95.
[30] J.R. Simões-Moreira, Adiabatic Evaporation Waves, Ph. D. Thesis, Rensselaer Polytechnic Institute, Troy, NY, USA, 1994.
[31] J.R. Simões-Moreira, Oblique evaporation waves, Shock Waves 10 (4) (2000) 229–234.
[32] J.R. Simões-Moreira, J.E. Shepherd, Evaporation waves in superheated dodecane, J. Fluid Mech. (382) (1999) 63–86.
[33] K. Okuyama, J.H. Kim, S. Mori, Y. Iida, Boiling propagation of water on a smooth film heater surface, Int. J. Heat Mass Transf. 49 (2006) 2207–2214.
[34] J.E. Shepherd, S. McCahan, J. Cho, Evaporation wave model for superheated liquids, in: G.E.A. Meyer, P.A. Thompson (Eds.), Adiabatic Waves in Liquid-Vapor Systems, Springer Verlag, Berlin, 1990.

[35] J.R. Simões-Moreira, S. McCahan, J.E. Shepherd, Complete evaporation waves, ASME Fluid Engineering Conference Washington DC, 1993.
[36] P.A. Thompson, D.A. Sullivan, On the possibility of complete condensation shock waves in retrograde fluids, J. Fluid Mech. 70 (4) (1975) 639–649.
[37] J.R. Simões-Moreira, Flashing in a vertical tube–video 1.12.1 and video 1.12.2, in: J.R. Thome (Ed.), Engineering Data Book III (2004-2010).
[38] J.R. Simões-Moreira, Simple modeling of evaporation waves, Euromech Colloquium 376 Waves in Two-Phase Flow, Istanbul, Turkey, 1998.